

## Full Paper

**Derived (Mutated)–Types of TRPV6 Channels Elicit Greater Ca<sup>2+</sup> Influx Into the Cells Than Ancestral-Types of TRPV6: Evidence From *Xenopus* Oocytes and Mammalian Cell Expression System**Yuka Sudo<sup>1,2,3</sup>, Kiyotaka Matsuo<sup>2</sup>, Tomoyuki Tetsuo<sup>2</sup>, Satoshi Tsutsumi<sup>2</sup>, Masamichi Ohkura<sup>4</sup>, Junichi Nakai<sup>4</sup>, and Yasuhito Uezono<sup>1,2,3,\*</sup>*Departments of*<sup>1</sup>*Molecular and Cellular Biology and*<sup>2</sup>*Pharmacology, Nagasaki University Graduate School of Biomedical Sciences, Nagasaki 852-8523, Japan*<sup>3</sup>*Cancer Pathophysiology Division, National Cancer Center Research Institute, Tokyo 104-0045, Japan*<sup>4</sup>*Saitama University Brain Science Institute, Saitama 338-8570, Japan*

Received June 29, 2010; Accepted August 26, 2010

**Abstract.** The frequency of the allele containing three derived nonsynonymous SNPs (157C, 378M, 681M) of the gene encoding calcium permeable TRPV6 channels expressed in the intestine has been increased by positive selection in non-African populations. To understand the nature of these SNPs, we compared the properties of Ca<sup>2+</sup> influx of ancestral (in African populations) and derived-TRPV6 (in non-African populations) channels with electrophysiological, Ca<sup>2+</sup>-imaging, and morphological methods using both the *Xenopus* oocyte and mammalian cell expression systems. Functional electrophysiological and Ca<sup>2+</sup>-imaging analyses indicated that the derived-TRPV6 elicited more Ca<sup>2+</sup> influx than the ancestral one in TRPV6-expressing cells where both channels were equally expressed in the cells. Ca<sup>2+</sup>-inactivation properties in the ancestral- and derived-TRPV6 were almost the same. Furthermore, fluorescence resonance energy transfer (FRET) analysis showed that both channels have similar multimeric formation properties, suggesting that derived-TRPV6 itself could cause higher Ca<sup>2+</sup> influx. These findings suggest that populations having derived-TRPV6 in non-African areas may absorb higher Ca<sup>2+</sup> from the intestine than ancestral-TRPV6 in the African area.

**Keywords:** TRPV6, calcium channel, fluorescence resonance energy transfer (FRET), electrophysiology

**Introduction**

The genes encoding the transient receptor potential cation channel subfamily V (vanilloid) members 5 and 6 (*TRPV5* and *TRPV6*) are expressed in a wide variety of tissues, with the highest level found in kidney and intestine, respectively. Both *TRPV5* and *TRPV6* encode six-transmembrane proteins that assemble into homotetramers to form Ca<sup>2+</sup>-selective membrane pores (Fig. 1) (1–3). Main Ca<sup>2+</sup> balance in the body is regulated by absorption through TRPV6 from the intestine and reabsorption and excretion through TRPV5 from renal tubules

(1–3). Because TRPV6 is involved in the rate-limiting step of dietary calcium absorption, genetic variation of the TRPV6 gene could affect dietary Ca<sup>2+</sup> absorption as well as Ca<sup>2+</sup> balance in the body. In the TRPV6 gene, a pattern of positive selection was observed in a 115-kb region of chromosome 7q34-35, which contains four genes, namely *KEL*, *TRPV5*, *TRPV6*, and *EPHB6* (4–6). This positive selection signature was observed in non-African populations but not in Africans (4, 5). In *TRPV6*, three derived nonsynonymous single nucleotide polymorphisms (SNPs) (157C, 378M, 681M) were in almost complete linkage disequilibrium and nearly fixed in non-African populations (see Fig. 1) (4, 6). A recent study indicated that the rate of TRPV6 protein evolution is significantly accelerated in the human lineage, but only for a haplotype comprised of a set of derived alleles at

\*Corresponding author. uezonoy0404@me.com

Published online in J-STAGE on October 8, 2010 (in advance)

doi: 10.1254/jphs.10169FP

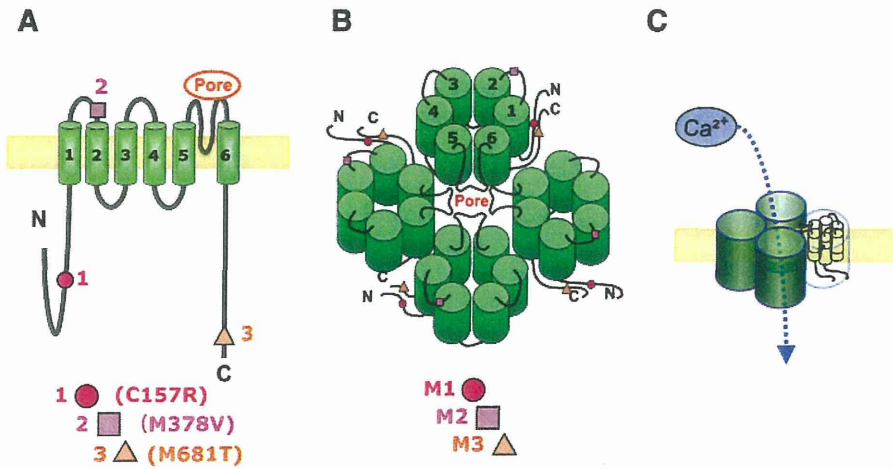


**Fig. 1.** Schema of ancestral- and derived (mutated)-TRPV6 channels. **A:** position of amino acid changes in ancestral- and derived (157C, 378M, 681M)-TRPV6 and their three-dimensional model (**B**). Pore: estimated pore-forming region in the TRPV6 channels. **C:** Extracellular  $\text{Ca}^{2+}$  enters into the pore in tetramerized TRPV6 channels.

the sites of C157R, M378V, and M681T. In addition, these three SNPs have high posterior probabilities of being targets for directional selection (5, 6). These results suggest that the derived-TRPV6 is a strong candidate for positive selection in non-African populations. It is possible that such amino acid changes contribute to confer functional changes in the TRPV6 channels and it is likely that derived-TRPV6 having such an amino acid change might be beneficial for non-African populations.

The present study was thus designed to investigate functional differences between derived non-African TRPV6 and ancestral African TRPV6. To this end, we performed *in vitro* analysis to compare the capability of  $\text{Ca}^{2+}$  influx into the cells in derived-TRPV6 to that in the ancestral-TRPV6 with a set of experiments including electrophysiological assay,  $\text{Ca}^{2+}$ -imaging analyses, and morphological studies to detect efficacy of multimeric (possibly tetrameric) channel formation by visual fluorescence resonance energy transfer (FRET) analysis, recently performed in our laboratory (7–9). Our electrophysiological,  $\text{Ca}^{2+}$ -imaging, and FRET analyses using individual TRPV6 channel-expressing cells showed that it is likely that the derived-TRPV6 has the capability to absorb a much greater amount of  $\text{Ca}^{2+}$  from the intestine than the ancestral-TRPV6.

## Materials and Methods

### Drugs and chemicals

Gentamicin and sodium pyruvate were purchased from Sigma (St. Louis, MO, USA). Other chemicals used in the study were of analytical grade and obtained from Nacalai Tesque (Kyoto).

### Construction of TRPV6 expression vectors

The complete coding region of the *TRPV6* gene was amplified from human placental cDNA (Clontech,

Mountain View, CA) using the primers 5'-GCCGAATTC GAGACAGGAGACGGGACCTCTACA-3' [an *EcoRI* recognition site (underlined) was introduced artificially] and 5'-GCCAAGCTTACCTCTGGGTGTTTGGTTTT TGT-3' [a *HindIII* recognition site (underlined) was introduced artificially]. The amplification was performed in 25  $\mu\text{l}$  of a mixture of 1  $\times$  buffer and 0.5 U of Phusion High-Fidelity DNA polymerase (New England BioLabs, Espoo, Finland). The temperature profile was denaturation at 98°C for 30 s, followed by 35 cycles of denaturation at 98°C for 7 s, annealing at 68°C for 30 s, and extension at 72°C for 75 s. The PCR product was digested with *EcoRI* and *HindIII* and then ligated into a pGEM-He-Juel vector. The sequence of the insert was confirmed by DNA sequencing using internal primers. DNA sequencing was performed with an ABI Prism 310 genetic analyzer (Applied Biosystems, Foster City, CA, USA). The vectors containing the ancestral-TRPV6 were constructed by use of a QuikChange Multi Site-Directed Mutagenesis Kit (Stratagene, La Jolla, CA, USA) using the derived-TRPV6 as the template. The temperature profile for mutagenesis was denaturation at 95°C for 1 min, followed by 30 cycles of denaturation at 95°C for 1 min, annealing at 55°C for 1 min, and extension at 65°C for 12 min. The mismatch primers used were MP157 (5'-TTCCGCCGTAGTCCCCGCAACCTCATCTA C-3'), MP378 (5'-TTCAGGAAGCCTACGTGACCCC TAAGGACG-3'), and MP681 (5'-CCTGTCCCTTCT ACGCCCTCAGTGTCTCG-3'). The sequences of the mutants were verified by sequencing. For construction of the fluorescent protein-fused TRPV6, we used the brighter variant of the cyan fluorescent protein Cerulean (10), which was kindly donated by Dr. D.W. Piston (Vanderbilt University, Nashville, TN, USA) and the brighter variant of the yellow fluorescent protein Venus (11), which was generously given to us by Dr. T. Nagai (Hokkaido University, Hokkaido). The TRPV6-Cerulean

and TRPV6-Venus in each ancestral- and derived-TRPV6 were generated by ligating the channel cDNAs into Hind III sites into the corresponding sites of Cerulean and Venus cDNAs.

#### *Construction of G-CaMP2-NT expression vector*

To visualize intracellular Ca<sup>2+</sup> concentration ([Ca<sup>2+</sup>]<sub>i</sub>) beneath the plasma membrane, we created a pN1-G-CaMP2-NT vector carrying the novel plasma membrane-targeted Ca<sup>2+</sup>-sensor G-CaMP2-NT, in which a targeting signal for attachment to the plasma membrane (LCCMRRTKQVEKNDQKI, deduced amino-acid residues in single-letter codes) (12) was fused at the N-terminus end of G-CaMP2 (GenBank accession no. DQ381402) (13). The cDNA sequence for the targeting signal was amplified by PCR. The PCR primers, designed to anneal themselves, were as follows: 5'-GGAGATCTG GATCCGATATCCGCCACCATGCTGTGCTGTAT GAGAAGAACCAAACAGG-3' and 5'-GGGTCGAC AATCTTTTGGTCCTCATCATTCTTTTCAACCTG TTTGGTTCTTCTACATACAGC-3'. The 0.09-kb PCR product was digested with *Bgl*III and *Sal*I and ligated with the 1.25-kb *Sal*I-*Not*I fragment from pN1-G-CaMP2 (13) and with the 3.94-kb *Bgl*III-*Not*I vector fragment from pN1-G-CaMP (14). The construct was verified by sequencing.

#### *Oocyte preparation and cRNA injection*

Immature V and VI oocytes from *Xenopus* were dissociated enzymatically as described previously (15). Isolated oocytes were incubated at 18°C in ND96 medium (96 mM NaCl, 2 mM KCl, 1.8 mM CaCl<sub>2</sub>, 1 mM MgCl<sub>2</sub>, and 5 mM HEPES, pH 7.4) containing 2.5 mM sodium pyruvate and 50 mg/ml gentamicin. For expression in *Xenopus* oocytes, all cDNAs for the synthesis of cRNAs were subcloned into the pGEM-He-Juel vector, which provided the 5'- and 3'-untranslated regions of the *Xenopus* β-globin RNA, ensuring a high level of protein expression in the oocytes (16). Each of the cRNAs was synthesized with a mCAP mRNA Capping Kit and with a T7 RNA polymerase in vitro Transcription Kit (Ambion, Austin, TX, USA) from the respective linearized cDNAs (7–9). For measurement of TRPV6-mediated currents induced by extracellular Ca<sup>2+</sup>, cRNA for the ancestral- or derived-TRPV6 (each 5 ng) was injected into oocytes. The final injection volume was <50 nl in all cases. Oocytes were incubated in ND96 and used 3–8 days after injection as reported previously (15).

#### *Electrophysiological recording with oocyte system*

Electrophysiological recordings were performed using the two-electrode voltage clamp technique with a Gene-clamp 500 amplifier (Axon Instruments, Foster City, CA,

USA) at room temperature. Oocytes were clamped at –60 mV and continuously superfused with nominally Ca<sup>2+</sup>-free ND96 buffer in a 0.25-ml chamber at a flow rate of 5 ml/min. Voltage recording microelectrodes were filled with 3 M KCl, and their tip resistance was 0.6–2.0 MΩ. Currents were continuously recorded and stored using MacLab (AD Instruments, Castle Hill, NSW, Australia) on a Macintosh computer, as described previously (7, 17).

#### *Mammalian cell culture and transfection*

Baby hamster kidney (BHK) cells or human embryonic kidney (HEK) 293T cells were grown in Dulbecco's modified Eagle's medium (DMEM) supplemented with 10% fetal bovine serum (FBS), penicillin (100 U/ml), and streptomycin (100 mg/ml) at 37°C in a humidified atmosphere of 95% air–5% CO<sub>2</sub>. BHK cells were used for fluorescent imaging studies, and HEK293T cells were used for the patch clamp study. BHK cells were seeded at a density of 1 × 10<sup>5</sup> cells per 35-mm glass-bottomed culture dish (Fluoro Physiotech, Tokyo) for 24 h. All cDNAs for transfection of mammalian cells were subcloned into pcDNA3.1(–) (Invitrogen, San Diego, CA, USA). Cells were used for analysis approximately 24 h after transfection. For patch clamp recordings of HEK293T cells, 0.2 μg of cDNAs for ancestral- or derived-TRPV6-Venus with 0.1 μg of G-CaMP2-NT was transfected. For Ca<sup>2+</sup> imaging with BHK cells, 0.2 μg of each channel with 0.1 μg of G-CaMP2-NT cDNA was transfected. For Western blotting of HEK293T cells, 0.2 μg of ancestral- or derived-TRPV6 (see *Western blot analysis* section) was also transfected.

#### *Electrophysiological recordings with HEK293T cells*

For electrophysiological recordings, we basically followed the procedures of Bodding et al. (18, 19). Briefly, HEK293T cells on coverslips were transfected with one TRPV6-Venus, transferred to the recording chamber, and kept in a modified Ringer's solution (145 mM tetraethylammonium chloride, 10 mM CaCl<sub>2</sub>, 10 mM CsCl, 2.8 mM KCl, 2 mM MgCl<sub>2</sub>, 10 mM HEPES, adjusted to pH 7.2 with NaOH). Patch clamp experiments were conducted in the tight-seal whole cell configuration using an EPC-7 amplifier (HEKA, Tokyo). Recording microelectrodes were filled with the standard internal solution (145 mM cesium glutamate, mM HEPES, 8 mM NaCl, 1 mM MgCl<sub>2</sub>, 2 mM MgATP, adjusted to pH 7.2 with CsOH) and their tip resistance was 2 to 3 MΩ. Currents were filtered using an 8-pole Bessel filter at 2.9 kHz. Cells for patch clamp experiments were identified by visualizing the Venus fluorescence with an inverted fluorescence microscope. Current–voltage (IV) relationships were measured by application of voltage-steps at a hold-

ing potential of  $-10$  mV from  $-110$  to  $30$  mV in  $10$ -mV increment of  $200$ -ms duration at  $0.5$  Hz using pClamp software (Axon Instruments). Currents were measured at the end of pulse during the last  $40$  ms of each pulse. Membrane potentials were corrected for  $10$ -mV liquid junction potentials. All experiments were carried out at room temperature ( $20^{\circ}\text{C} - 23^{\circ}\text{C}$ ); internal solutions were kept on ice to minimize ATP hydrolysis. The data were analyzed using Clampfit (Axon Instruments) and Sigma-Plot (SPSS, Inc., Chicago, IL, USA).

#### Western blot analysis

Goat polyclonal TRPV6 antibody (N-16) and actin antibody were obtained from Santa Cruz Biotechnology (Santa Cruz, CA, USA). An anti-rabbit polyclonal GFP antibody that recognizes GFP as well as Cerulean and Venus was kindly provided by Dr. N. Saito of Kobe University (Kobe). *Xenopus* oocytes were injected with the ancestral- or derived-TRPV6 cRNA, and HEK293T cells were transfected with ancestral- or derived-TRPV6/TRPV6-Venus. For protein isolation, oocytes or HEK293T cells expressing each TRPV6 were sonicated and solubilized in PRO-PREP protein extraction buffer containing a combination of protease inhibitors (iNtRON Biotechnology, Sungnam, Korea) for  $1$  h at  $4^{\circ}\text{C}$ , as reported previously (8, 9). The mixtures were centrifuged ( $15,000$  rpm,  $30$  min), and the supernatants were stored at  $-80^{\circ}\text{C}$  until Western blot analysis. The supernatants were dissolved in Laemmli sample buffer containing  $0.1$  M dithiothreitol, subjected to  $7.5\%$  SDS-polyacrylamide gel electrophoresis (PAGE), transferred to polyvinylidene fluoride (PVDF) membranes, and subjected to immunoblotting using the polyclonal TRPV6 antibody (1:200). This was followed by a secondary goat anti-IgG conjugated with horseradish peroxidase (HRP) at 1:2,000 dilution for detection and then reacted with Western blot chemiluminescence detection reagents (Nacalai Tesque). In some experiments, the anti-rabbit GFP polyclonal antibody (1:10,000) was followed by a secondary rabbit anti-IgG with HRP (1:5,000) and the actin antibody (1:10,000) was followed by a secondary goat anti-IgG with HRP (1:10,000).

#### $\text{Ca}^{2+}$ imaging of TRPV6-expressing BHK cells with the $\text{Ca}^{2+}$ -sensor G-CaMP2-NT

$\text{Ca}^{2+}$  imaging was performed using BHK cells coexpressing each of the TRPV6 with the  $\text{Ca}^{2+}$ -sensor G-CaMP2-NT, which localizes mostly just beneath the plasma membrane (13, 20). Cells placed in  $35$ -mm glass-bottom dishes ( $1 \times 10^5$  cells/dish) were transfected with  $0.2$   $\mu\text{g}$  of the ancestral- or derived-TRPV6 together with  $0.1$   $\mu\text{g}$  G-CaMP2-NT. The fluorescence of G-CaMP2-NT was continuously recorded at a wavelength of  $510$  nm,

and the fluorescence intensity in each whole cell was measured. Then, the extracellular medium was changed from a nominally  $\text{Ca}^{2+}$ -free buffer to a buffer containing  $18$  mM  $\text{Ca}^{2+}$ . Data were calculated with the LSM510 META software (Carl Zeiss, Jena, Germany) and expressed as intensity of fluorescence ( $510$  nm) and compared with fluorescence intensity of the cells in the nominally  $\text{Ca}^{2+}$ -free medium.

#### FRET analysis by confocal microscopy

Protein complex formation of TRPV6-Cerulean and TRPV6-Venus was analyzed using FRET capability of the confocal microscope. BHK cells cultured in  $35$ -mm glass-bottomed dishes were cotransfected with  $0.2$   $\mu\text{g}$  of Cerulean- or Venus-tagged ancestral-TRPV6 and/or derived-TRPV6. A  $63\times$  magnification,  $1.25$ -aperture oil immersion objective was used with a pinhole for visualization. Cerulean and Venus were both excited by a  $458$ -nm laser, and images of live cells were taken by placing the dish onto the stage of the confocal microscope LSM510 META, as described previously (7–9).

#### Photobleaching and calculation of FRET efficiency

To confirm FRET between Cerulean and Venus, we monitored FRET-acceptor photobleaching in BHK cells coexpressing TRPV6-Venus and TRPV6-Cerulean, as reported previously (7–9). In brief, FRET was measured by imaging Cerulean before and after photobleaching Venus with a  $514$ -nm argon laser at  $100\%$  power intensity. As a control, we examined the FRET efficiency of at least three areas of unbleached membranes in the same cell. FRET efficiency was then calculated using the equation  $E = (I_D - I_{DA}) / I_D$ , where  $I_{DA}$  is the peak of donor (Cerulean) emission in the presence of the acceptor and  $I_D$  is the peak in the presence of the sensitized acceptor, as described previously (7–9, 21).

#### Statistical analysis of functional analyses

Data are expressed as means  $\pm$  S.E.M. Differences between two groups were examined for statistical significance using Student's *t*-test. Prism software (GraphPad Software, La Jolla, CA, USA) was used to analyze data for statistical significance and to analyze data and fit curves for extracellular  $\text{Ca}^{2+}$  dose-responses. A *P* value less than  $0.05$  denoted the presence of a statistically significant difference.

## Results

#### Effect of three nonsynonymous SNPs in TRPV6 channels on the properties of $\text{Ca}^{2+}$ influx

*Xenopus* oocytes are a useful system for functional electrophysiological analysis of ion channels and  $\text{Ca}^{2+}$ -

mobilizing G protein-coupled receptors (15, 22) and also have been used for an analysis of TRPV6-channel function by detecting Ca<sup>2+</sup>-activated Cl<sup>-</sup>-channel activity endogenously expressed in oocytes (23). When TRPV6 is activated by addition of extracellular Ca<sup>2+</sup>, increases in [Ca<sup>2+</sup>]<sub>i</sub> stimulate Ca<sup>2+</sup>-activated Cl<sup>-</sup> channels to elicit robust Cl<sup>-</sup> currents (23), suggesting that the amplitude of the Cl<sup>-</sup> currents reflected the increases in [Ca<sup>2+</sup>]<sub>i</sub>, resulting from TRPV6-mediated Ca<sup>2+</sup> influx. In oocytes expressing ancestral-TRPV6, a change from the nominally Ca<sup>2+</sup>-free buffer to the 1.8 mM Ca<sup>2+</sup>-containing ND96 buffer elicited dual phase inward currents (Fig. 2A), as reported previously in oocytes expressing TRPV6 (23) and oocytes directly injected with CaCl<sub>2</sub> beneath the plasma membrane (24). We confirmed that the currents elicited by addition of Ca<sup>2+</sup> were composed of outward Cl<sup>-</sup> currents through activation of the Ca<sup>2+</sup>-activated Cl<sup>-</sup>

channels, based on the current-voltage relationship curve as shown by other investigators (23) and our previous study (15). In oocytes expressing the derived-TRPV6, switching to the 1.8 mM Ca<sup>2+</sup>-containing buffer induced much robust Cl<sup>-</sup> currents compared with the oocytes expressing the ancestral-TRPV6 (Fig. 2: A and B). In oocytes injected with H<sub>2</sub>O instead of TRPV6 cRNAs, no apparent currents were observed (Fig. 2: A and B). When varying concentrations of extracellular Ca<sup>2+</sup> (0.2, 0.4, 0.9, 1.8, and 9 mM) were applied, derived-TRPV6 showed higher Ca<sup>2+</sup>-influx activity than ancestral-TRPV6 in all the concentrations used (Fig. 2C). Western blot analysis using actin antibody as the internal standard showed that both groups of oocytes expressed almost the same amount of proteins (Fig. 2D). Band intensities obtained with TRPV6 antibody showed that both channels were similarly expressed in the oocytes (Fig. 2D).

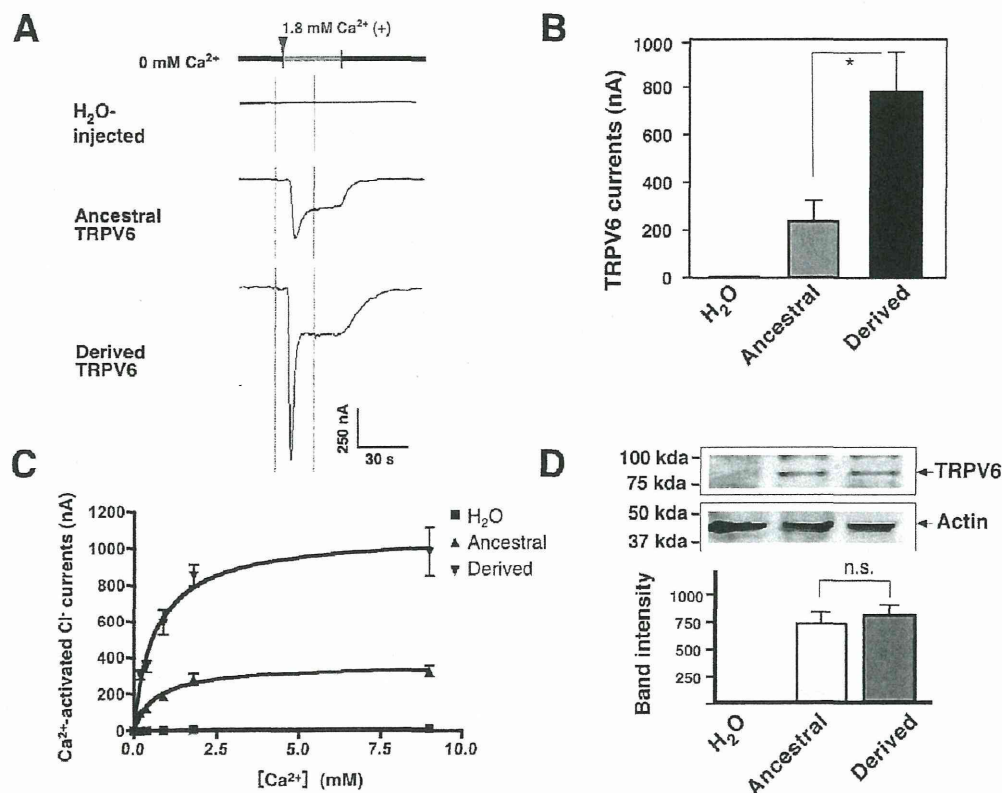


**Fig. 2.** Effects of addition of extracellular Ca<sup>2+</sup> on the activity of Ca<sup>2+</sup>-activated Cl<sup>-</sup> channels in *Xenopus* oocytes expressing ancestral- or derived-TRPV6. **A:** Typical tracings of Ca<sup>2+</sup>-activated Cl<sup>-</sup> currents by addition of ND96 buffer containing 1.8 mM CaCl<sub>2</sub> in oocytes with or without expressing ancestral- or derived-TRPV6 at holding potential of -60 mV. **B:** Ancestral- or derived-TRPV6-mediated Ca<sup>2+</sup>-activated Cl<sup>-</sup> currents. Data are the mean ± S.E.M. values from 10 each oocytes. Ancestral: ancestral-TRPV6, Derived: derived-TRPV6. Significantly different (\**P* < 0.05) from the mean of the ancestral TRPV6. **C:** Concentration-dependent activation of Ca<sup>2+</sup>-activated Cl<sup>-</sup> currents in oocytes expressing ancestral- or derived-TRPV6. Note that oocytes expressing derived TRPV6 show superior Cl<sup>-</sup> currents in all Ca<sup>2+</sup> concentration used. **D:** Western blot analysis of the TRPV6 proteins extracted from oocytes. H<sub>2</sub>O: oocytes injected with H<sub>2</sub>O, Ancestral: oocytes injected with ancestral-TRPV6, Derived: oocytes injected with derived-TRPV6. Top: bands detected with TRPV6 antibody (83 kda). Middle: bands detected with actin antibody (42 kda) with the same Western-blot membranes. Bottom: summary of the band intensity with TRPV6 antibody. Not significant (n.s) band intensity was detected with TRPV6 antibody between oocytes expressing ancestral- or derived-TRPV6.

The differences between  $\text{Ca}^{2+}$ -activated  $\text{Cl}^-$  currents observed in oocytes expressing ancestral- and derived-TRPV6 are assumed to be due to different amounts of  $\text{Ca}^{2+}$  influx through the individual TRPV6. To further directly compare the functional differences between ancestral- and derived-TRPV6, we performed patch clamp analysis with HEK293T cells transfected with the fluorescent protein Venus-tagged ancestral- or derived-TRPV6. To confirm whether TRPV6-Venus and non-

tagged TRPV6 have similar properties, we injected cRNAs encoding ancestral-TRPV6-Venus or derived-TRPV6-Venus into oocytes. In the electrophysiological experiments, we found that both tagged-TRPV6 elicited  $\text{Ca}^{2+}$ -activated  $\text{Cl}^-$  current similar to those of non-tagged ancestral- or derived-TRPV6 (ancestral type, TRPV6  $248.2 \pm 32$  nA, TRPV6-Venus  $278.0 \pm 29$  nA; derived type, TRPV6  $740.6 \pm 90.3$  nA, TRPV6-Venus  $820.8 \pm 85.0$  nA,  $n = 10$  each) at holding potential of  $-60$  mV.

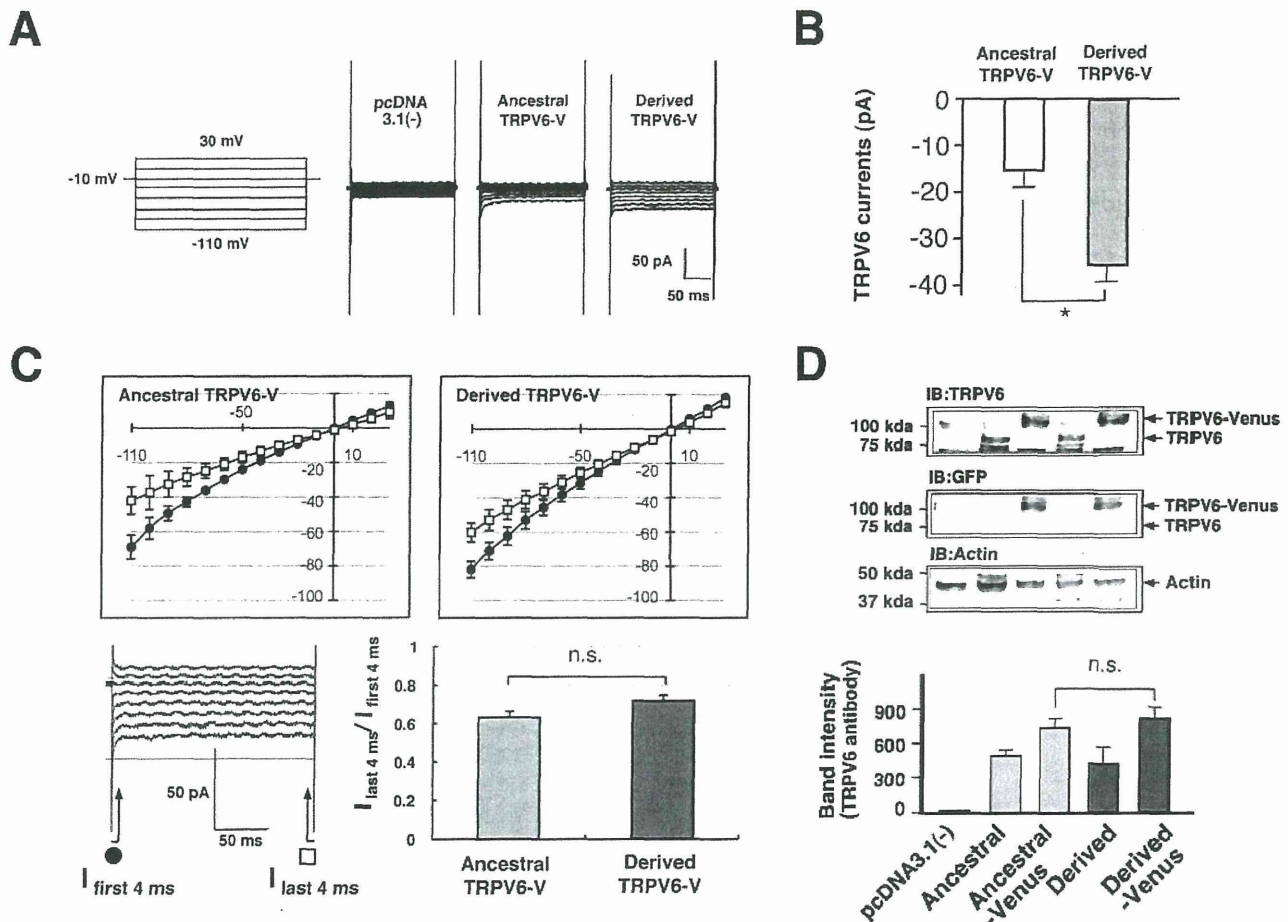


**Fig. 3.** Current-voltage relationship of the  $\text{Ca}^{2+}$ -induced inward current  $I_{\text{TRPV6}}$  in HEK293T cells transfected with the pcDNA3.1(-) vector alone, ancestral-, or derived-TRPV6-Venus (TRPV6-V). **A:** Left, voltage step command. Currents were evoked by voltage steps between  $-110$  to  $30$  mV (200-ms duration) with the holding potential of  $-10$  mV. Right, representative currents evoked by the voltage steps after maximum activation of the inward currents by  $10$  mM  $\text{Ca}^{2+}$  in pcDNA3.1(-) vector-, ancestral-TRPV6-Venus-, or derived-TRPV6-Venus-expressing cells. **B:** Extracellular  $\text{Ca}^{2+}$ -induced inward currents through ancestral- or derived-TRPV6-V after subtraction of control currents obtained from cells expressing pcDNA3.1(-) alone. Data are the mean  $\pm$  S.E.M. values ( $n = 17$ , ancestral-TRPV6-V;  $n = 21$ , derived-TRPV6-V). Significantly different ( $*P < 0.05$ ) from the mean of the ancestral-TRPV6-V. **C:** Current-voltage relationships (IV curves) for the ancestral- or derived forms of TRPV6-V measured from 4-ms average at the start (4 ms after the beginning of the voltage step,  $I_{\text{first 4 ms}}$ ) and the end of the pulse (4 ms prior to the end of the voltage step,  $I_{\text{last 4 ms}}$ ) as indicated by the arrows ( $n = 8$  for each group of the cells). The voltage-step protocol was the same as in panel A. Summary of the ratio of  $I_{\text{last 4 ms}}/I_{\text{first 4 ms}}$  (Right bottom panel C). n.s.: No significant difference of  $I_{\text{last 4 ms}}/I_{\text{first 4 ms}}$  ratio between cells expressing ancestral- and derived-TRPV6-V. **D:** Western blot analysis of the TRPV6 proteins extracted from HEK293T cells. Top, immunoblotted with antibody against TRPV6. Middle, immunoblotted with antibody against GFP. TRPV6-V (110 kDa), TRPV6 (83 kDa). Bottom, immunoblotted with antibody against actin, and summarized data of band intensities immunoblotted with TRPV6 antibody ( $n = 4$ ). n.s.: No significant difference between band intensities with cells expressing ancestral- and derived-TRPV6-V.

In control HEK293T cells transfected with pcDNA3.1(-) vector alone, inward currents ( $-37.17 \pm 6.83$  pA,  $n = 13$ ) were observed to the switch holding potential from  $-10$  to  $-110$  mV. This is probably due to endogenously expressed Ca<sup>2+</sup>-permeable TRPV channels (possibly TRPV5 and/or TRPV6) in HEK293T cells. In the cells transfected with ancestral-TRPV6-Venus, a robust increment in the Ca<sup>2+</sup>-induced inward current was observed ( $-51.37 \pm 3.25$  pA,  $n = 17$ ) (Fig. 3: A and B) similarly as previously reported (18, 19). Further increases in Ca<sup>2+</sup>-induced inward currents were observed in cells transfected with derived-TRPV6-Venus ( $-70.0 \pm 2.64$  pA,  $n = 21$ ) (Fig. 3: A and B). I-V relationship

analysis showed an inward rectification profile, and a fast initial decay was observed in both ancestral-TRPV6-Venus- and derived-TRPV6-Venus-expressing cells, particularly at the negative voltage of  $< -40$  mV (Fig. 3C, Top panel). This decrease in Ca<sup>2+</sup> entry from the first 4-ms currents after beginning of the voltage-steps to the end of 4-ms currents during the 200-ms voltage-step at  $-110$  mV is based on channel inactivation induced by increase in  $[Ca^{2+}]_i$  (18, 19). TRPV6 channels are characterized by their Ca<sup>2+</sup>-induced inactivation during hyperpolarizing voltage steps, and this Ca<sup>2+</sup>-dependent feedback inhibition affects the properties of TRPV6 channels (3, 18, 19). We thus compared the efficacy of the Ca<sup>2+</sup>-

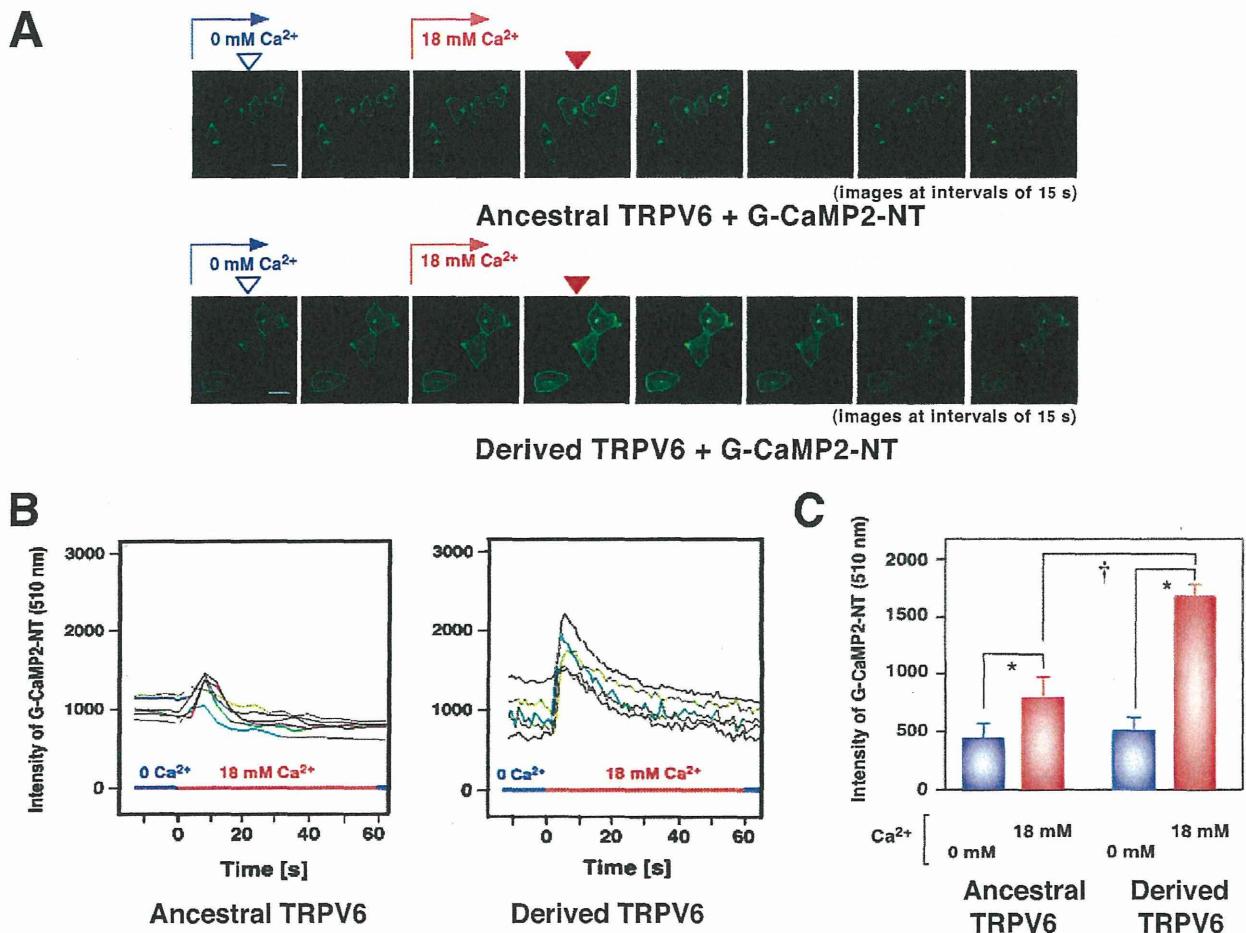


**Fig. 4.** Ca<sup>2+</sup> imaging of BHK cells coexpressing individual TRPV6 together with the Ca<sup>2+</sup>-sensor protein G-CaMP2-NT. **A:** Time course of visualized G-CaMP2-NT intensity following addition of 18 mM CaCl<sub>2</sub> to the buffer of BHK cells coexpressing ancestral-TRPV6 (Top) or derived-TRPV6 (Bottom). Calibration bar = 10  $\mu$ m. **B:** Time course of intensity of G-CaMP2-NT fluorescence (510 nm) in cells transfected with ancestral-TRPV6 (Left) or derived-TRPV6 (Right) together with G-CaMP2-NT. The transfected cells were stimulated with 18 mM extracellular Ca<sup>2+</sup> for 60 s. Note that similar steep increases and decay of fluorescence intensity were observed. G-CaMP2-NT intensity was measured at individual whole cell area with the Carl Zeiss Meta software. **C:** Intensity of G-CaMP2-NT fluorescence (510 nm) in BHK cells expressing ancestral- or derived-TRPV6. Fluorescence intensities were measured as in panel B before (open arrowhead) and after (closed arrowhead) the addition of Ca<sup>2+</sup> in panel A. Data are the mean  $\pm$  S.E.M. values of 6 independent experiments ( $n = 36 - 40$ ). Significantly different ( $*P < 0.05$ ) from the intensity without Ca<sup>2+</sup> and significantly different ( $^{\dagger}P < 0.05$ ) from the intensity in cells expressing ancestral-TRPV6.

inactivation profiles between cells expressing ancestral- and derived TRPV6-Venus. As shown in the right bottom panel of Fig. 3C, the ratio of the currents ( $I_{\text{last } 4 \text{ ms}}/I_{\text{first } 4 \text{ ms}}$ ) at the voltage step of  $-110 \text{ mV}$  was not significantly different, suggesting that there were no differences in the  $\text{Ca}^{2+}$ -inactivation processes between the ancestral- and derived-TRPV6 channels. Western blot analysis using TRPV6 antibody and the GFP antibody that can detect Venus protein showed that each group of cells expressed almost the same amount of individual TRPV6-Venus or TRPV6 transfected with ancestral-TRPV6, ancestral-TRPV6-Venus, derived-TRPV6, or derived-TRPV6-Venus cDNAs (Fig. 3D). With the same membranes we

confirmed that almost same amounts of proteins were eluted in each lane by detecting actin protein as an internal standard (Fig. 3D).

We further sought to examine increases in  $[\text{Ca}^{2+}]_i$  induced by activation of ancestral- or derived-TRPV6 channels. In BHK cells coexpressing ancestral-TRPV6 together with G-CaMP2-NT, which allows visualization of changes in  $[\text{Ca}^{2+}]_i$  beneath the plasma membrane (14, 20 and see Materials and Methods), addition of  $18 \text{ mM}$   $\text{Ca}^{2+}$  increased the intensity of green fluorescence beneath the plasma membrane and the cytosol (Fig. 4A). In cells expressing the derived-TRPV6 instead of the ancestral-TRPV6, a much brighter green fluorescence was observed

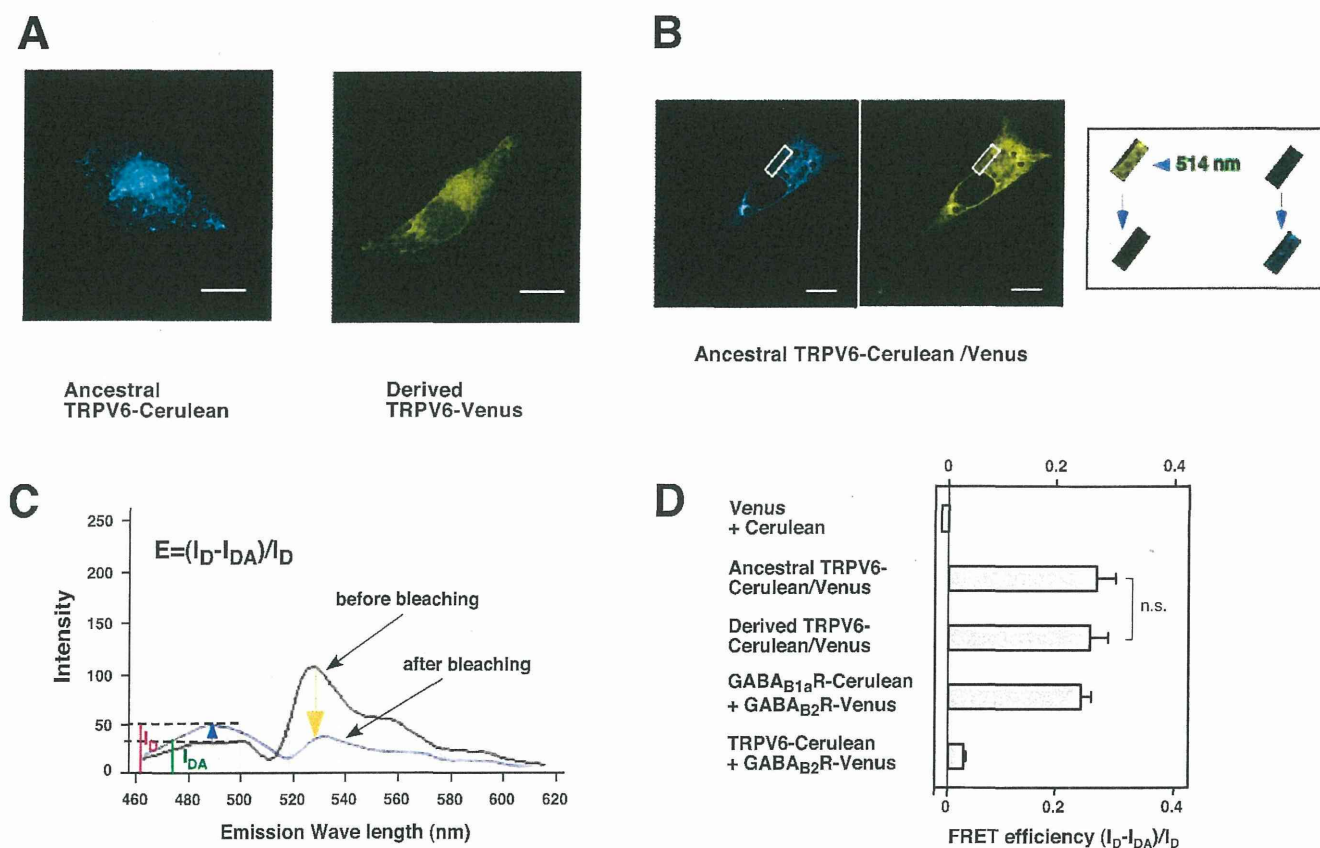


**Fig. 5.** Confocal imaging and FRET analysis of multimer formation between ancestral- and derived-TRPV6 in BHK cells coexpressing a combination of ancestral-TRPV6-Cerulean/Venus or derived-TRPV6-Cerulean/Venus. **A:** Visualization of ancestral-TRPV6-Cerulean and derived-TRPV6-Venus at the plasma membrane and cytosol in BHK cells. Similar fluorescence was observed in cells expressing ancestral-TRPV6-Venus or derived-TRPV6-Cerulean (data not shown). Calibration bar =  $10 \mu\text{m}$ . **B:** Changes in fluorescence induced by acceptor photobleaching (15-s application at  $514 \text{ nm}$ ) in BHK cells coexpressing ancestral-TRPV6-Cerulean/Venus. **C:** Emission spectra from a BHK cell before and after Venus photobleaching as indicated in panel B. Note the increase of the Cerulean peak emission ( $488 \text{ nm}$ ) following photobleaching of Venus ( $528 \text{ nm}$ ). The mathematical equation used for calculating the FRET efficiency ( $E$ ) is also shown.  $I_{DA}$ , peak of donor emission in the presence of acceptor;  $I_D$ , peak of donor emission in the presence of sensitized acceptor. **D:** Comparison of FRET efficiency for ancestral-TRPV6-Cerulean/Venus and derived-TRPV6-Cerulean/Venus. The combination of Venus + Cerulean and GABA<sub>B1a</sub>R-Cerulean + GABA<sub>B2</sub>R-Venus pairs was used as negative and positive controls for protein-protein interaction, respectively. Each bar represents the mean  $\pm$  S.E.M. of FRET efficiency in independent experiments using three regions of interest per BHK cell in six cells ( $n = 18$ ). n.s.: No significant difference of FRET efficiency between ancestral-TRPV6-Cerulean/Venus and derived-TRPV6-Cerulean/Venus.



(Fig. 4: A – C), demonstrating that the derived-TRPV6 transported larger amounts of Ca<sup>2+</sup> into the cells than the ancestral one. The time course of [Ca<sup>2+</sup>]<sub>i</sub> shown in Fig. 4B demonstrated that steep increases and fast inactivation of [Ca<sup>2+</sup>]<sub>i</sub> were observed in both of the TRPV6 channels, which were typical properties of TRPV6 channels.

*FRET analysis after acceptor photobleaching in BHK cells coexpressing ancestral- or derived-TRPV6*

TRPV6 is considered to form homotetramers by itself or heterotetramers with TRPV5 (25). Using FRET measurement after acceptor photobleaching techniques, previously performed in our laboratories (7 – 9), we investigated whether the ancestral-TRPV6 and derived-TRPV6 form multimers (possibly tetramers). Fluorescence from the ancestral-TRPV6-Cerulean and derived-TRPV6-Venus was diffuse in the cells (Fig. 5A). The ancestral-TRPV6-Venus and derived-TRPV6-Cerulean fluorescence were also similarly diffuse in the cells, (data not shown). Acceptor photobleaching analysis of BHK cells coexpressing the ancestral-TRPV6-Cerulean/Venus showed a decrease in Venus intensity associated with an increase in Cerulean fluorescence (Fig. 5: B and C), indicating formation of a protein complex between the ancestral-TRPV6-Cerulean/Venus molecules, as shown in our previous studies (7 – 9). The FRET efficiency of the ancestral-TRPV6-Cerulean/Venus and that of the derived-TRPV6-Cerulean/Venus were similar (Fig. 5D), suggesting similar properties of multimer formation in both the ancestral- and derived-TRPV6. As a positive control, we measured FRET efficiency of the formation of functional GABA<sub>B</sub> receptors (GABA<sub>B</sub>R) composed of GABA<sub>B1a</sub>R and GABA<sub>B2</sub>R, which are known to form a heterodimer (7, 8). In contrast, almost no FRET was observed (Fig. 5D) in cells coexpressing Cerulean + Venus or the ancestral-TRPV6-Cerulean + GABA<sub>B2</sub>R-Venus, indicating specific multimer formation of TRPV6 channels.

## Discussion

In the TRPV6 gene, a pattern of positive selection was observed in a 115-kb region of chromosome 7q34-35 (4 – 6). *TRPV6* has three derived nonsynonymous SNPs (157C, 378M, 681M), which were in almost complete linkage disequilibrium and nearly fixed in non-African populations (Fig. 1) (4, 6). These three SNPs have high posterior probabilities of being targets for directional selection (5, 6), suggesting that the derived-TRPV6 having three SNPs is a strong candidate for positive selection in non-African populations. Changes in such amino acids might have contributed to confer functional changes in

the TRPV6 channels, and it is likely that derived-TRPV6 having such an amino acid change would be beneficial for non-African populations.

The present study showed by several different functional methods that the capability for Ca<sup>2+</sup>-influx increase in the derived-TRPV6 is greater than that of the ancestral-TRPV6 (Figs. 2 – 4). Oocytes expressing derived-TRPV6 showed much more robust Ca<sup>2+</sup>-activated Cl<sup>-</sup> currents in response to Ca<sup>2+</sup> addition than those expressing ancestral-TRPV6, even though the protein expression levels of both channels were almost the same. Patch-clamp analysis also demonstrated that HEK293T cells expressing derived-TRPV6 but not ancestral-TRPV6 elicited much more Ca<sup>2+</sup> influx, although both channel proteins were expressed equally. Furthermore, Ca<sup>2+</sup>-imaging analysis demonstrated that extracellular Ca<sup>2+</sup>-induced [Ca<sup>2+</sup>]<sub>i</sub> increase was higher in cells expressing derived-TRPV6 than those expressing the ancestral one. In addition, Ca<sup>2+</sup>-dependent feedback inhibition as demonstrated by Ca<sup>2+</sup>-induced TRPV6 inactivation did not differ between ancestral- and derived-TRPV6. Finally, properties and efficiency of TRPV6-channel assembly to multimer channels were not significantly different between derived- and ancestral-TRPV6. Collectively these results indicate that the derived-TRPV6 itself has a greater capability to increase Ca<sup>2+</sup> influx than ancestral-TRPV6.

On the other hand, Suzuki et al. (26) reported results different from our functional analysis data on ancestral- and derived-TRPV6; they showed that the ancestral-TRPV6 was more Ca<sup>2+</sup>-permeable than the derived one with the <sup>45</sup>Ca<sup>2+</sup>-uptake assay using the *Xenopus* oocyte expression system. The reason for this discrepancy is unclear at present, but possible reasons for this difference are the different experimental design and extracellular Ca<sup>2+</sup> concentration they used; they measured <sup>45</sup>Ca<sup>2+</sup> influx to the oocytes at a single extracellular Ca<sup>2+</sup> concentration (0.2 mM) as a functional TRPV6 assay. According to their report, the ancestral-TRPV6 may have higher Ca<sup>2+</sup>-uptake properties at low Ca<sup>2+</sup> concentration. However, this is unlikely because our results using different (0.2 – 9 mM) concentrations of extracellular Ca<sup>2+</sup> showed that derived-TRPV6 elicited higher Ca<sup>2+</sup>-influx activity (measured by Ca<sup>2+</sup>-activated Cl<sup>-</sup> currents) at all the tested concentrations, including 0.2 mM Ca<sup>2+</sup>. We performed functional comparison of derived- and ancestral-TRPV6 with a combination of assay methods, but it will be necessary, nonetheless, to make detailed functional analyses of ancestral- and derived-TRPV6 to better understand the driving forces behind their functional differences.

As TRPV6 channels are involved in the rate-limiting step of dietary calcium absorption (1, 2), it seems that individuals having the derived-TRPV6 could absorb more dietary calcium from the intestine than individuals

having the ancestral one. It is well known that TRPV6 expression levels are associated with the activity of vitamin D<sub>3</sub>, which requires ultraviolet light for its activation (1, 2). These findings may have implications for adaptation to calcium deficiency due to vitamin D<sub>3</sub> insufficiency, conferring an advantage to individuals with derived-TRPV6 over individuals with the ancestral-TRPV6, especially in areas at high latitudes with low ultraviolet light exposure. This observation may provide a plausible explanation for the selective force for an increased frequency of the derived-TRPV6 with three nonsynonymous SNPs outside Africa.

Another possible explanation for the different Ca<sup>2+</sup>-influx property between ancestral- and derived-TRPV6 is that some type of genetic event that impacted calcium homeostasis might have occurred in non-African populations but not in African populations. This explanation assumes that the importance of calcium uptake differs between the African and non-African populations. As speculated by Akey et al. (5), the presence of two different types of TRPV6 channels might be beneficial, and some form of balancing selection may have been acting on this locus in Africa (5). Indeed, a recent study suggests that the calcium ion is integral to proper immune function, and TRPV6 has been implicated as one of the modulators of T-cell activation (27). We speculate that if the signature of gene selection may have been related to pathogen susceptibility, individuals carrying the derived-TRPV6 channels in the non-African area may have resistance against some types of pathogens, while individuals carrying the ancestral-TRPV6 in Africa area may have resistance against other types of pathogens. Interestingly, a recent report showed that the A563T variation of renal epithelial TRPV5, channels that reabsorb Ca<sup>2+</sup> into renal tubules, was expressed among African Americans, and this variant elicited enhanced Ca<sup>2+</sup> influx by affecting the Ca<sup>2+</sup>-permeation pathway compared with its wild type (28). They speculate that the A563T variant may contribute to the superior ability of renal Ca<sup>2+</sup> conservation in African Americans (28).

SNPs in derived-TRPV6 were in almost complete linkage disequilibrium and almost no populations of TRPV6 with one or two positions of SNP (5), and it is not known at present which mutation(s) in the three derived-TRPV6 is/are important for their higher ability to permeate Ca<sup>2+</sup>. Such experiments using site-directed derived-TRPV6 with only one changed amino acid (TRPV6-157C, TRPV6-378M, TRPV6-681M) are ongoing studies in our laboratory.

In conclusion, we showed that derived-TRPV6 is capable of increasing TRPV6-mediated Ca<sup>2+</sup> influx, suggesting that individuals having the derived-TRPV6 could absorb more dietary calcium from the intestine than those

having the ancestral-TRPV6, which provide a possible selective advantage, promoting the spread of the advantageous haplotype outside Africa, including the European area.

### Acknowledgments

This work was supported by Grants-in-Aid for Scientific Research from the Ministry of Education, Culture, Sports, Science, and Technology of Japan (Y.U.); a grant from Daiichi Sankyo Pharmaceutical Co., Ltd. (Y.U.); Smoking Research Foundation (Y.U. and Y.S.); and a grant from Nagasaki University, Graduate School of Biomedical Sciences (Y.S.).

### References

- 1 van Abel M, Hoenderop JG, Bindels RJ. The epithelial calcium channels TRPV5 and TRPV6: regulation and implications for disease. *Naunyn Schmiedebergs Arch Pharmacol.* 2005;371:295–306.
- 2 Nijenhuis T, Hoenderop JG, Bindels RJ. TRPV5 and TRPV6 in Ca(2+) (re)absorption: regulating Ca(2+) entry at the gate. *Pflugers Arch.* 2005;451:181–192.
- 3 Venkatachalam K, Montell C. TRP channels. *Annu Rev Biochem.* 2007;76:387–417.
- 4 Akey JM, Eberle MA, Rieder MJ, Carlson CS, Shriver MD, Nickerson DA, et al. Population history and natural selection shape patterns of genetic variation in 132 genes. *PLoS Biology.* 2004;2:e286.
- 5 Akey JM, Swanson WJ, Madeoy J, Eberle M, Shriver MD. TRPV6 exhibits unusual patterns of polymorphism and divergence in worldwide populations. *Hum Mol Genet.* 2006;15:2106–2113.
- 6 Stajich JE, Hahn MW. Disentangling the effects of demography and selection in human history. *Mol Biol Evol.* 2005;22:63–73.
- 7 Uezono Y, Kanaide M, Kaibara M, Barzilai R, Dascal N, Sumikawa K, et al. Coupling of GABAB receptor GABAB2 subunit to G proteins: evidence from *Xenopus* oocyte and baby hamster kidney cell expression system. *Am J Physiol Cell Physiol.* 2006;290:C200–C207.
- 8 Kanaide M, Uezono Y, Matsumoto M, Hojo M, Ando Y, Sudo Y, et al. Desensitization of GABA(B) receptor signaling by formation of protein complexes of GABA(B) subunit with GRK4 or GRK5. *J Cell Physiol.* 2007;210:237–245.
- 9 Hojo M, Sudo Y, Ando Y, Minami K, Takada M, Matsubara T, et al.  $\mu$ -Opioid receptor forms a functional heterodimer with cannabinoid CB<sub>1</sub> receptor: electrophysiological and FRET analysis. *J Pharmacol Sci.* 2008;108:308–319.
- 10 Rizzo MA, Springer GH, Granada B, Piston DW. An improved cyan fluorescent protein variant useful for FRET. *Nat Biotechnol.* 2004;22:445–449.
- 11 Nagai T, Ibata K, Park ES, Kubota M, Mikoshiba K, Miyawaki A. A variant of yellow fluorescent protein with fast and efficient maturation for cell-biological applications. *Nat Biotechnol.* 2002;20:87–90.
- 12 Zacharias DA, Violin JD, Newton AC, Tsien RY. Partitioning of lipid-modified monomeric GFPs into membrane microdomains of live cells. *Science.* 2002;296:913–916.
- 13 Lee MY, Song H, Nakai J, Ohkura M, Kotlikoff ML, Kinsey SP,